JOURNAL OF SOLID STATE CHEMISTRY 2, 472–482 (1970)

Crystallographic Shear in Oxygen-Deficient Rutile: An Electron Microscope Study

J. S. ANDERSON AND R. J. D. TILLEY

Inorganic Chemistry Laboratory, University of Oxford, Oxford, England

Received May 22, 1970

Electron microscopy, electron diffraction, and direct lattice imaging show that extended defects are important in substoichiometric TiO_2. Planar faults on {132} in near-stoichiometric TiO_2 are identified as shear planes, of different orientation from the shear in the Magnéli phases. $TiO_{1.99}$ (just outside the monphasic range at 1000°C) has a complex structure with twinning and unmixing into TiO_2-like and oxygen deficient regions. The latter show imperfectly ordered {132} shear planes at 30–40 Å spacings, corresponding to elements of oxides Ti_nO_{2n-1} with $30 < n < 40$. In crystals of the Magnéli phases Ti_5O_9 to Ti_8O_{15}, with {121} shear planes, occasional stacking mistakes and coherent domain intergrowths of several members of the series are found. The growth and rearrangement of shear planes is considered in relation to the diffusion mechanisms proposed by Wadsley and Andersson and by Anderson and Hyde.

The work described here is an investigation of the defect structure of oxygen-deficient rutile. The mechanism by which crystalline compounds accommodate a significant deviation from ideal stoichiometry is one of the important problems of solid state chemistry and physics, since in ionic solids at least (e.g., metallic oxides) the concentration of true point defects is too small to account fully for nonstoichiometric behaviour (*1*). There is now ample evidence that interactions between defects lead to clustering, ordering or to the elimination of point defects by the process termed *crystallographic shear* (*2*), although the formalism of point defect theory is often still used in discussing the behaviour, and particularly the electronic properties, of solids without proper regard to the structural validity of the model.

Rutile readily undergoes some loss of oxygen under reducing conditions at high temperature. The apparent range of stoichiometry seems to depend on the purity of the material, but Alcock, Steele, and Zador (*3*, *4*) have determined the lower limit of composition at 1000°C as $TiO_{1.933}$ for very pure rutile that had been floating zone refined in oxygen. It has been disputed whether the oxygen deficiency should be interpreted in terms of oxygen vacancies or titanium interstitials, but the attainable deficiency is almost certainly too high to be ascribed to random point defects.

Reduction of rutile below the composition $TiO_{1.9}$ produces a succession of intermediate phases $Ti_nO_{2n-1}(4 \leqslant n < 10)$, derived from rutile by crystallographic shear (*5*). In these structures, the octahedral coordination of the cations is preserved, but the coordination polyhedra are more compactly linked to shear faces, along certain crystallographic directions, thereby decreasing the anion–cation ratio (Fig. 1). Crystallographic shear virtually displaces one slab of crystal with respect to a neighbouring slab, along a defined (*hkl*) plane, the *shear plane*, the displacement being defined by a *shear vector*, which approximates to a lattice vector of the parent structure when allowance is made for distortions in the fused octahedral groups. The shear vector must have a component normal to the shear plane in order to give rise to a change in chemical composition; a shear vector lying wholly in the shear plane produces a stacking fault or antiphase boundary (*6*). In the series of compounds Ti_4O_7 to Ti_9O_{17}, the shear plane is $(12\bar{1})$, but it has been pointed out that other shear planes are possible —for example $(13\bar{2})$ (*6*). The present work shows the importance of this alternative shear system as a means of eliminating defects in the early stages of

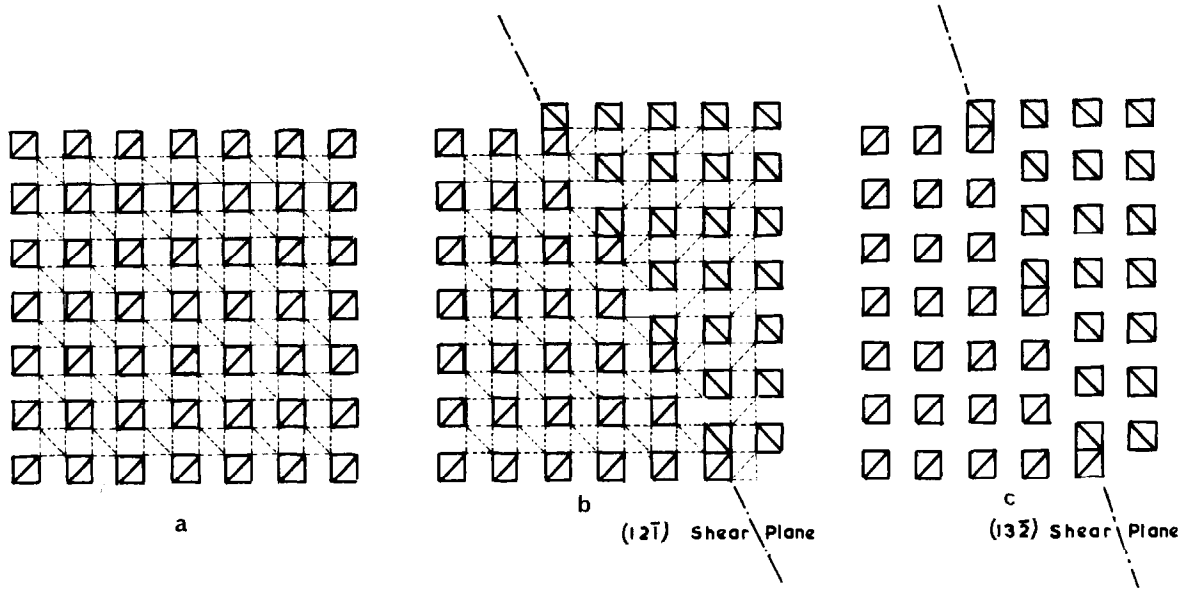

FIG. 1. Crystallographic shear in rutile (a) TiO_2, (001) projection, schematic. Full lines: octahedra at level $Z = 0$; dotted lines: octahedra at $Z = \frac{1}{2}$. (b) Result of shear $\frac{1}{2}\langle a0c\rangle$ on (12$\bar{1}$) plane. Octahedra at $Z = 0$ and $Z = \frac{1}{2}$ shown. (c) result of shear $\frac{1}{2}\langle a0c\rangle$ on (13$\bar{2}$) plane.

reduction of rutile. After this work had started, Bursill, Hyde, Terasaki, and Watanabe (*7*) reported the existence of an extensive new series of ordered intermediate oxides, also with the general formula Ti_nO_{2n-1}, based on (13$\bar{2}$) shear.

Formation of shear phases of definite composition implies that the slabs of rutile structure between successive shear planes are absolutely regular in breadth. To a first approximation, neither the structure in the shear plane itself, nor the slightly perturbed rutile of the slab between a pair of shear planes, is affected by the shear plane spacing. Attainment of regular spacings thus involves subtle long range ordering effects; disorder or randomised coherent intergrowth of slabs of different widths should lead to only a small increase in the free energy of a crystal. Nevertheless, from the evidence of X-ray diffraction and chemical equilibrium, the (12$\bar{1}$) shear plane phases appear to behave as fully ordered compounds of fixed composition (*5*, *8*).

Electron diffraction and electron microscopy afford a sensitive means of investigating these materials. An isolated shear plane is a planar fault; an ordered shear phase has a regular array of such faults defining a new superlattice. The rutile-based shear phases are triclinic; the normal to the $(hkl)_R$[1] shear planes lies along the c^* direction of the reciprocal lattice of the new structure, and is given, for a phase Ti_nO_{2n-1}, by the relation

$$c^* = nd^*_{hkl}.$$

The orientation and spacing of shear planes can thus be derived from electron diffraction data; randomization of spacings or coherent intergrowth of thin lamellae with a common shear plane but different shear plane spacings (and therefore different compositions), is made evident by streaking along the c^* direction.

We record here observations on (a) very slightly oxygen deficient rutile, (b) rutile reduced just below the stable composition limit at 1000°C, and (c) crystals of the defined (12$\bar{1}$) series of intermediate phases. It must be emphasised that observations made at room temperature do not necessarily correspond to the equilibrium state at 1000°C, but may be modified by some displacement of equilibrium before short range diffusion processes become frozen during cooling. The stable composition range of rutile at low temperatures is certainly infinitesimal, so that the oxygen deficient material should, in principle, precipitate a lower oxide phase during cooling. The observed structural features may therefore be due in part to incomplete quenching of the high-temperature state. They at least demonstrate the facility with which crystallographic shear occurs, and they bear on the mechanism by

[1] The subscript attached to the symbol implies the (*hkl*) plane referred to in the original rutile structure.

which shear planes are introduced into and migrate within the crystals to form an ordered arrangement.

Experimental

Crystals of titanium oxides with compositions in the range TiO_2–$TiO_{1.5}$ were prepared in several ways. To produce crystals of very slightly non-stoichiometric TiO_2, "Specpure" titanium dioxide (Johnson and Matthey) was heated for 5 days at 1200°C in a platinum tube, which was sealed up within a silica ampoule under about one-third of an atmosphere of hydrogen chloride to promote mineralisation. A more reduced sample, of composition close to $TiO_{1.99}$, was prepared from a single crystal of very pure TiO_2 by coulometric titration of oxygen out of the crystal at 1000°C. The starting material was a slice cut from a boule of zone-refined TiO_2 and the final composition was just below the edge of the homogeneity range at 1000°C.[2] This sample had been cooled rather slowly in the solid-state galvanic cell used for the reduction.

Samples of the defined Magneli phases Ti_6O_{11}–Ti_8O_{15} were obtained from experiments on the growth of crystals by chemical vapour transport. Hydrogen chloride gas (or the mixture of HCl, H_2 and N_2 formed by introducing ammonium chloride into the transport system) was used as transport reagent. In contact with the oxide it establishes an equilibrium with gaseous $TiCl_4$, H_2, and H_2O which was self-buffering with respect to the chemical potential of oxygen. Transport was carried out in sealed silica tubes, in the temperature gradient 1100° → 950°C. Using a poorly crystalline sample of approximate composition Ti_7O_{13}, partial transport was effected in 4 days, and the untransported material was excellently recrystallised. Crystals from this residue were used for electron microscopy.

Samples for transmission microscopy were prepared by fracture. X-ray powder patterns were taken with a Guinier–Hagg focusing camera, using CuKα radiation.

Results

1. Slightly Reduced Rutile

This material, which was blue-black in colour, showed only rutile lines in its X-ray diffraction pattern. In the electron microscope, many fragments showed no defects other than occasional dislocations and damage due to fracture. However, some fragments contained planar boundaries which were usually fairly straight and separated from each other, rather than in clusters [Fig. 2(a)]. Analysis of diffraction patterns showed that these boundaries lay on {132} planes. They were identified as α-boundaries since their fringe patterns were symmetrical about the central fringe in bright field (*9*). We did not determine the displacement vector, since this was being studied by Hyde and Bursill (University of Western Australia), who have now (*10*), identified it as $\frac{1}{2}\langle 0, 0.95b, 0.95c\rangle$, corresponding essentially to the shear vector predicted for {132} shear planes. Fringe patterns of the faults are occasionally seen to change at some point on the fault [e.g., at A, Fig. 2(a)]. Dislocation contrast is also visible at that point. No evidence of diffuse scattering or superlattice reflections was seen in any diffraction pattern.

By focusing the electron beam after removing the condenser aperture, the α-boundaries could often be made to vanish [Fig. 2(b)]. This took place rapidly, the boundaries always contracting along their length. Boundaries terminating within the crystals were easily removed, contracting from the tip of the fault lying within the matrix, whereas faults that passed completely across the crystal were more stable. More intense heating under the same conditions produced new faults, again boundaries lying in several planes of the {132} group [Fig. 2(c)]. These boundaries grew into the crystal along their length and were usually initiated at the edge of the crystal. Faults could be made to grow in and out of the crystal repeatedly by altering the intensity of the electron beam.

Further intense heating resulted in the production of complex arrays of faults. Individual faults could be seen to move parallel to their length. Streaking appeared on diffraction patterns and was sometimes seen to lie along $\langle 121\rangle$ directions as well as along $\langle 132\rangle$ and ordered arrays of superlattice spots were occasionally observed. Under extreme conditions, the edges of the crystals contracted as if the crystal were fluid, and arrays of twins formed. Diffraction patterns were complex, often showed streaking, and could not be indexed on the basis of the rutile reciprocal lattice alone.

As indicated by the fringe contrast, the planar boundaries are α-boundaries, which are formed between two identical slabs of crystal, one of which is displaced with respect to another by the vector **R**. If **R** lies in the fault plane, the fault is of the stacking fault type; if **R** is at an angle to the fault plane it implies that the lattice has collapsed, and the fault

[2] We are indebted to Dr. B. C. H. Steele and Miss S. Zador, Department of Metallurgy, Imperial College, for providing this sample.

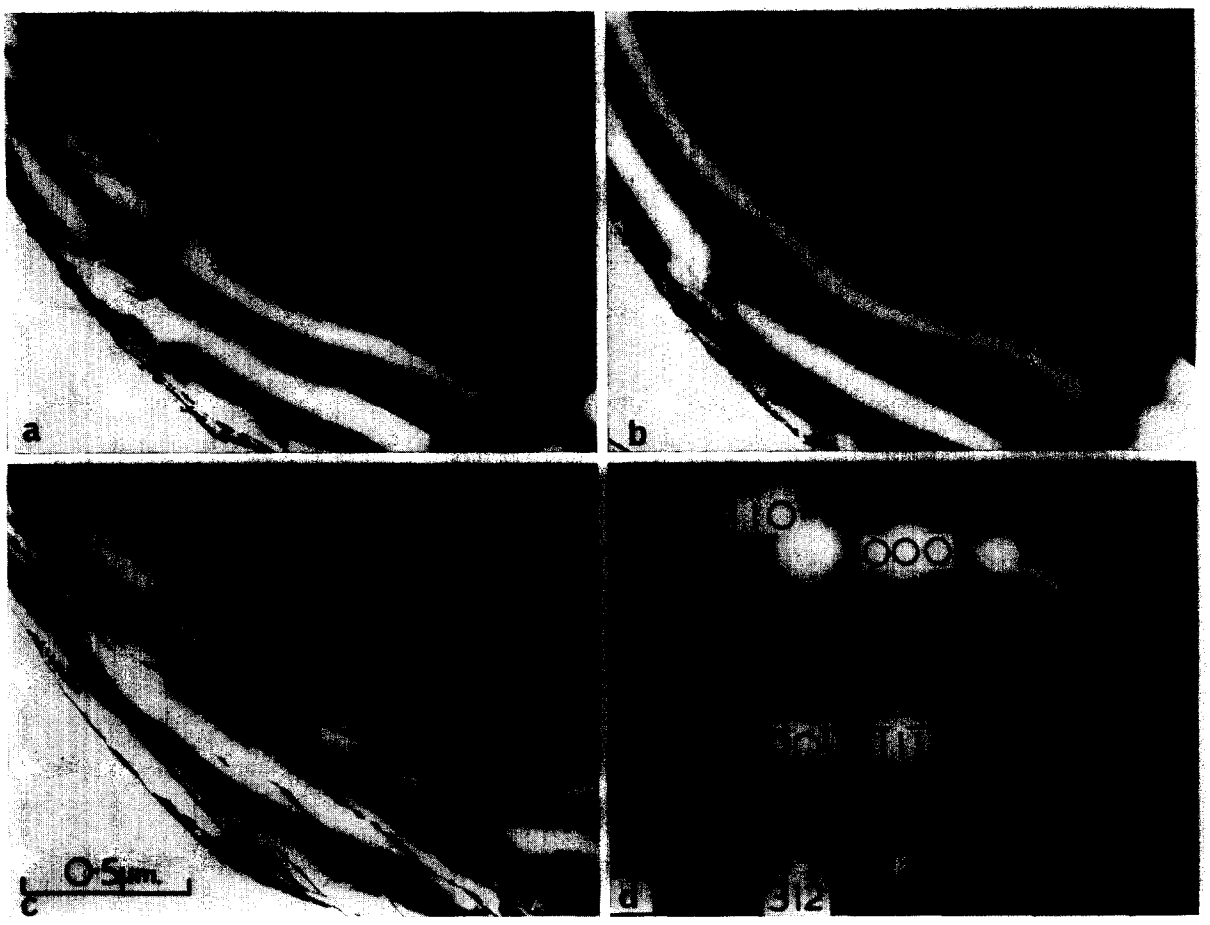

FIG. 2. Almost stoichiometric TiO_2 (a) as prepared, showing isolated planar faults, (b) after beam heating, showing disappearance of boundaries, (c) after further beam heating, introducing new boundaries. (d) is the diffraction pattern of (c) and shows streaking parallel to $(\bar{3}1\bar{2})$. Magnification of micrographs 75,000×.

is a shear plane corresponding to a change in composition.

Although there has been some doubt about the value of **R** for planar faults observed in rutile, there is evidence that they are associated with a change in stoichiometry (*11*, *12*, *13*). Other indirect evidence argues against identifying them as stacking faults. They do not lie in the known {110} slip planes of rutile and {132} planes are likely to be unsuitable for slip. Moreover, the faults have not been found in stoichiometric rutile even after severe mechanical stress accompanying fracture. Finally, the manner in which these faults anneal into and out of the crystal during beam heating is not typical of stacking faults. We have therefore assumed that the {132} faults are planes of crystallographic shear, and this assumption has been justified by the determination of **R**, by Hyde and Bursill (*10*).

These results suggest that deviation from stoichiometry in rutile is not, or not wholly, attributable to point defects, but is at least partially accommodated by crystallographic shear. Individual shear planes are formed, not in the {121} planes characteristic of the known homologous series of oxides (planar boundaries of {121} orientation were observed in no case), but on the alternative {132} planes.

Both the introduction of shear planes by beam heating and the way in which they annealed out of the crystal accord with the dislocation mechanism of Anderson and Hyde (*6*), but this does not explain the movement of faults parallel to themselves under intense beam heating; such movement is necessary if any ordered array is to be produced. The alternative diffusion mechanism postulated by Andersson and Wadsley (*14*) may well operate under these

conditions. For shear plane migration in rutile, this would entail the cooperative movement of titanium atoms, with the anion lattice unchanged.

The change of fringe contrast, as shown at A, Fig. 2(a), is probably due to an overlap of closely spaced, parallel shear planes (*11*, *15*). That such overlap occasionally occurs suggests that the occurrence and spacing of neighbouring shear planes is influenced by the force field around a shear plane. It could be regarded as an incipient ordering, and a pair of shear planes could be regarded as enclosing a lamella, one unit cell thick, of an oxide structure derived from rutile by {132} shear, with a composition defined by the spacing between the shear planes.

Streaking in the electron diffraction patterns is due to disorder in the region of the crystal that is diffracting the wave front (*16*). Isolated planar defects give rise to short streaks or spikes normal to the planar fault; large numbers of randomly spaced and oriented defects give rise to continuous streaking along the reciprocal lattice direction normal to the planes containing the defects. Thus the streaking shown in Fig. 2(d) is normal to the $(\bar{3}1\bar{2})$ planes shown in Fig. 2(c).

The occasional development of streaks along $\langle 121 \rangle$ directions suggests that disordered {121} shear planes are forming, although it is necessary to emphasise that any planar boundary on {121} (e.g., stacking faults) would have a similar effect. The appearance of distinct spots implies that a new regular structure is appearing; as these superlattice spots lie on the $\langle 121 \rangle$ streaking, it is likely that the disordered state causing streaking is becoming progressively ordered into a distinct structural type—for example, a coherent domain of one of the known {121} shear structures. Unfortunately, beam heating is difficult to control, so that it has not as yet been possible to obtain structural information about the processes whereby material containing {132} shear planes is converted to a material with at least partially ordered {121} shear planes.

The ultimate formation of a highly twinned structure is complex and appears to involve melting, or a quasiliquid state. The finely twinned form cannot be an equilibrium state in the sense of classical thermodynamics, and interfacial energy (e.g., strain arising from coherence between two structures) may well be important in the formation of the twinned lamellae. Moreover, because of the presence of the carbon support film close to the titanium oxide crystals, it is possible that carbon may be incorporated in the fluid stage, or may participate in reduction reactions.

2. $TiO_{1.99}$

Fragments of the black, coulometrically reduced single crystal of $TiO_{1.99}$ showed two distinct kinds of microstructure. In the first, there were complex arrays of planar faults [Fig. 3(a)]. Well-defined fine twinning was observed equally frequently [Fig. 3(b)] with boundaries lying approximately along $\{100\}_R$ and $\{010\}_R$ planes. A fine structure, on the scale of 100–200 Å in width, was often found within each twin. These fragments always gave complex diffraction patterns, with far more reflections than would be given by the basic rutile reciprocal lattice. Streaking was often observed, usually lying along $\langle 132 \rangle_R$ directions, but occasionally along $\langle 101 \rangle_R$ [Fig. 4(a),(b)], together with a tendency for the streaks to break up into superlattice spots corresponding to a long periodicity along $\langle 132 \rangle_R$.

Lattice fringe resolution, using the superlattice spots and streaking along $\langle 132 \rangle_R$, was used to clarify this microstructure, which was difficult to interpret using diffraction contrast alone. In Fig. 5(a), resolved lattice planes parallel to $(132)_R$ are seen in one set of a series of twins revealed by diffraction contrast, while the other set shows no fringes. It is apparent from the fringe patterns that the spacings are not completely uniform, and there are marked discontinuities of spacing that correspond to the ill-defined microstructure seen in diffraction contrast. The diffraction pattern of this region [Fig. 5(b)] shows several overlapping periodicities and background streaking, as would be expected from a poorly ordered array of planes.

Similar variations in fringe spacing were obtained from other crystal flakes, and a microdensitometer trace [Fig. 6(c)] revealed variations in spacing even in regions that at first sight appeared uniform [Fig. 6(a)]. Over wide areas, these $\{132\}_R$ fringes appeared to be grouped into bands of wider and narrower spacings (Fig. 7); a microdensitometer trace across these showed abrupt, rather than sinusoidal, fluctuations in spacing. The average fringe spacing of all resolved planes measured was about 34 Å, with extremes of 20 and 38 Å.

These planar features could not be annealed out of the crystal by beam heating. Intense heating did cause considerable reaction, however, and produced twins similar to those formed from nearly stoichiometric rutile. As with that material, the hard edge of the crystal changed shape and the crystal appeared to become almost fluid. The twins usually showed an internal fine structure, with considerable streaking in the diffraction patterns.

In Section 1 we have given reasons for identifying

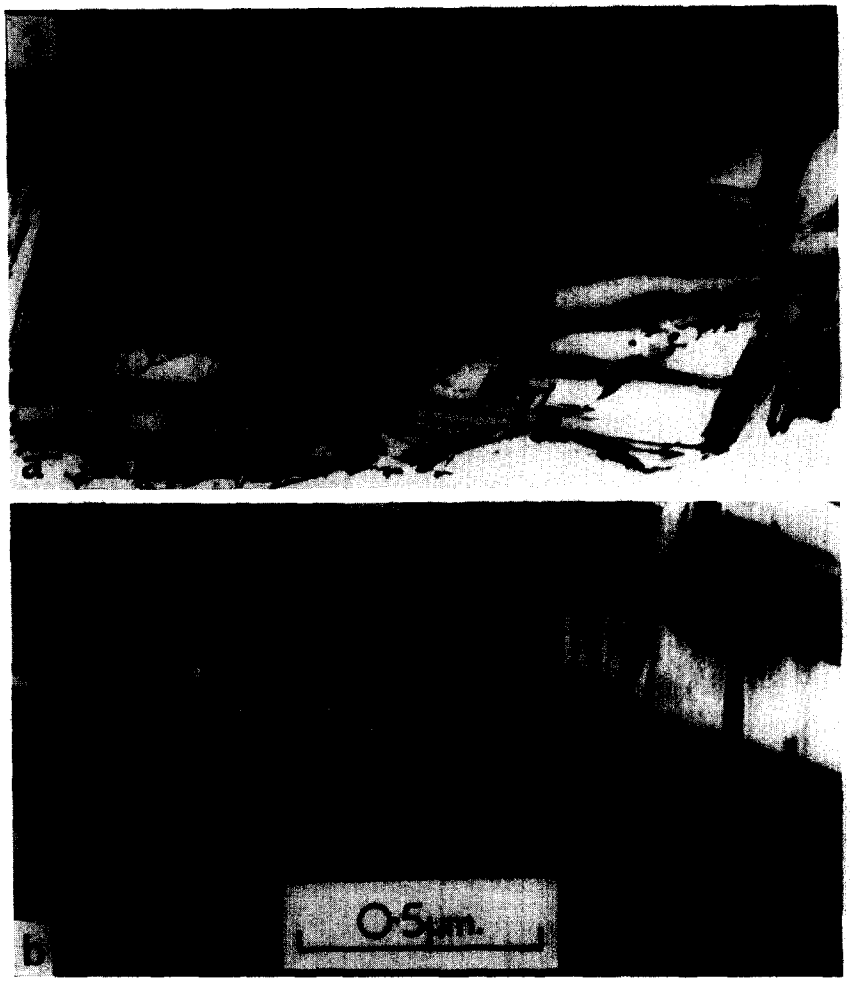

FIG. 3. (a) Irregular arrays of planar faults in $TiO_{1.99}$. (b) Complex fine twinning in $TiO_{1.99}$. Magnification 75,000×.

the $\{132\}_R$ α-boundaries with planes of crystallographic shear. In $TiO_{1.99}$ such planes occur in some regions at fairly wide and quite irregular spacings (Fig. 3a) whereas other regions show a closely spaced succession of such planes which is imperfectly ordered. An isolated shear plane constitutes a fault in the rutile structure; a perfectly regular succession of shear planes, however long its periodicity, defines a new, ordered intermediate compound Ti_nO_{2n-1}, as described by Hyde, Bursill, Terasaki, and Watanabe. Regions of crystal such as is shown in Fig. 5 can be regarded as disordered members of this series, with layers of parent structure of somewhat variable thickness enclosed between successive shear planes. In the examples shown, the values of n can be worked out as in the range 30–40. The irregularity shown in the microphotometer traces implies that, in many cases, one oxide structure may be present as a lamella only one unit cell thick, (measured along the c^* direction of the superlattice). The same kind of random but coherent intergrowth in a shear structure has been described by Allpress (*17*) for structures derived from Nb_2O_5. For $30 < n < 40$, the approximate composition of the crystal would be $TiO_{1.97}$ so that, for a mass balance, two-thirds of the crystal must have a composition close to TiO_2. This is the material represented by Fig. 3(a), with a low density of completely disordered faults.

The distribution of $\{132\}_R$ shear planes represents a variation of composition within the crystal, brought about either during the coulometric reduction at 1000°C or during cooling. As, with change of composition or temperature, such a crystal crosses the solvus line from a homogeneous area into a biphasic area of the equilibrium diagram, true equilibrium would be reached by formation of distinct crystals of the derivative lower oxide structure, but separation and ordering would be

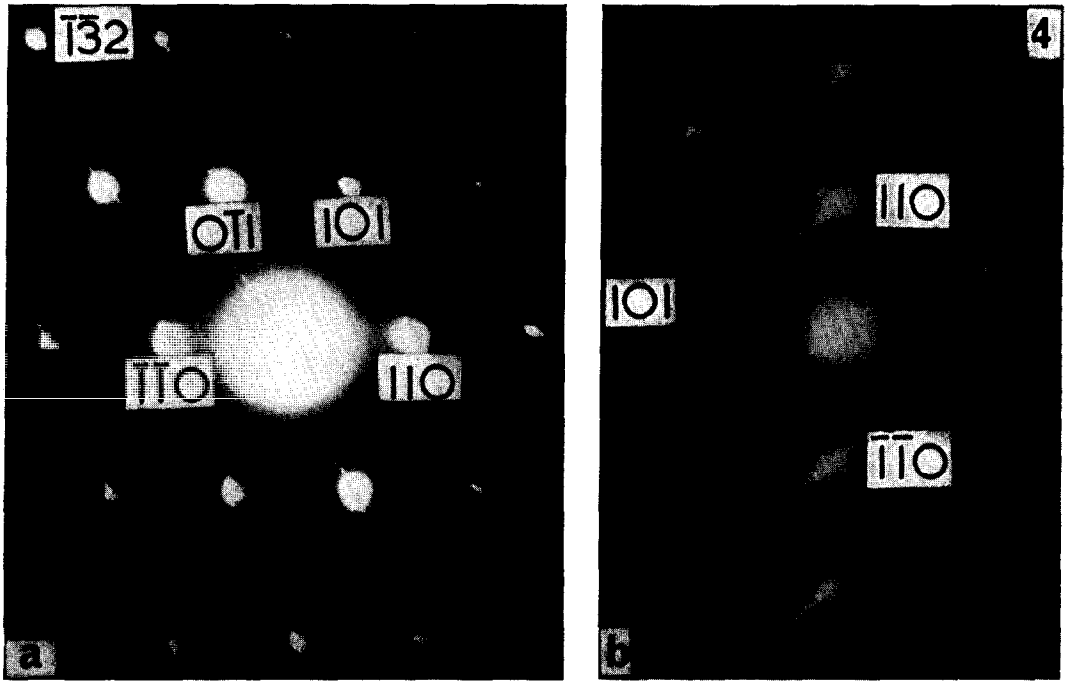

FIG. 4. Diffraction patterns from $TiO_{1.99}$ showing (a) streaking along ⟨132⟩ directions, and (b) streaking along ⟨132⟩ and ⟨101⟩ directions.

FIG. 5. (a) The same twins as in Fig. 3(b), one set showing resolved lattice planes. Note the imperfect spacing of the fringes. Poorly resolved fringes are seen in the other twin. Magnification 380,000×. (b) Diffraction pattern corresponding to (a).

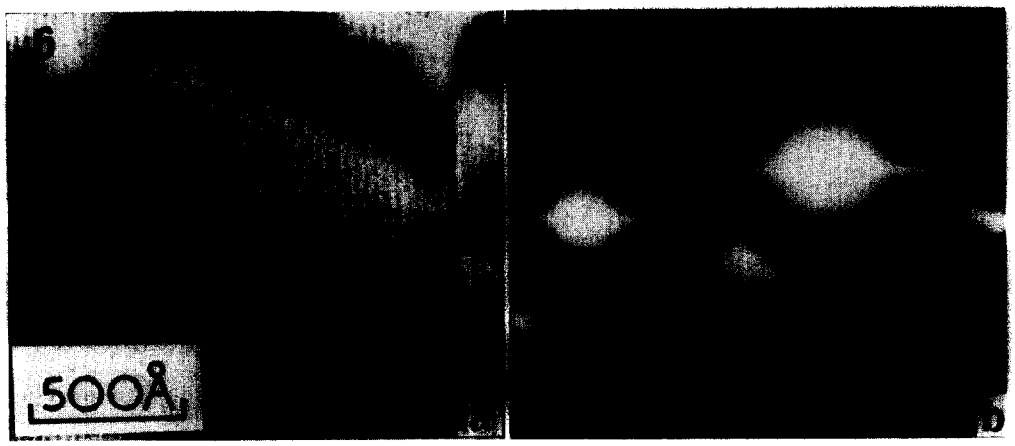

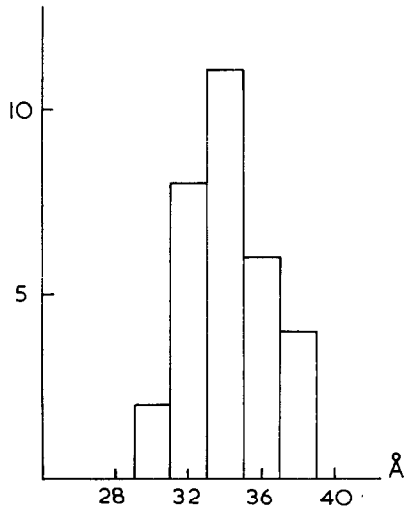

FIG. 6. (a) Resolved lattice fringes in $TiO_{1.99}$ imaged using the central beam and the streak adjacent to it shown in the diffraction pattern (b). (c) Part of a microdensitometer trace across the region in (a) and a histogram showing the fringe separation. Magnification of (a) 380,000×.

governed kinetically by the sluggish diffusion process. The structure observed is thus to be regarded as a frozen, transient state in the approach to equilibrium. The bands of alternating fringe spacings in Fig. 7(a) suggest a segregation into oxygen-rich and oxygen-poor regions, of 200–400 Å width, this width being governed by the diffusion length in the particular volume of crystal during the separation. In this respect it resembles the effect predicted for spinodal decompositions, but the observed distribution of spacings does not afford any evidence of a sinusoidal variation of composition.

Even where reduced material is in intimate contact with regions approximating to TiO_2, the spacing of arrayed fringes does not appear to exceed 40 Å. This suggests that long range interactions between shear planes, which underly the ordering, are not very effective beyond this distance. This would imply a composition around $Ti_{40}O_{79}$, for the highest effective member of the series Ti_nO_{2n-1}, although suitable annealing might

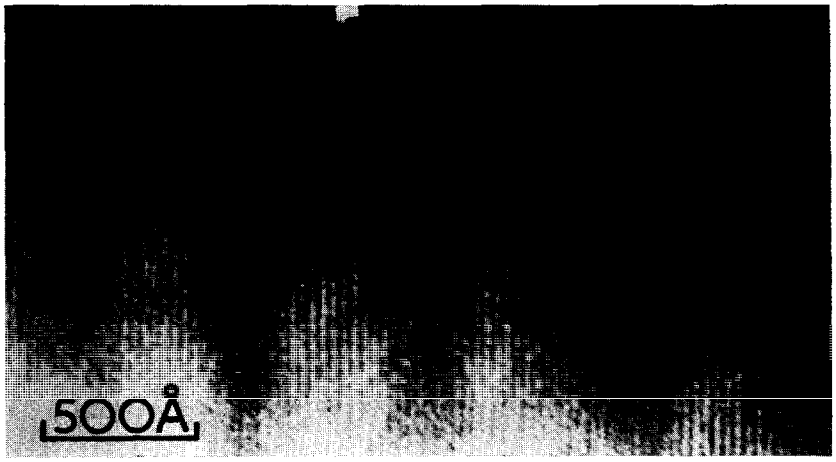

FIG. 7. $TiO_{1.99}$ showing regions containing resolved $(1\bar{3}2)$ planes and regions of TiO_2. Magnification 380,000×.

generate ordered, or nearly ordered, arrays of shear planes with an even smaller oxygen deficiency. Under realistic experimental conditions, however, slightly reduced rutile in the composition range TiO_2 to $TiO_{1.98}$ would be composed either of rutile with random $\{132\}_R$ shear planes or, at larger oxygen deficiences, regions of Ti_nO_{2n-1}, with $n \sim 30$–40, imperfectly ordered, in contact with or intergrown with, rutile containing shear planes. Point defects are presumably present at low concentration, and must be invoked for the unit steps of diffusion processes, but the observations imply that a deficit of oxygen is at least partially accommodated by extended defects before any new and identifiable lower oxide structure is formed.

The streaking shown on Fig. 4(b) raises the question whether $\{132\}_R$ planes are the only ones operative in this composition range. The evidence does not suffice to say whether the streaking is due to shear on $\{101\}_R$, but $\{101\}$ twin planes in substoichiometric rutile have been reported (*12*) and streaking may be due to these. However, the possibility of alternative shear planes should not be ruled out, particularly in the composition range near $TiO_{1.90}$ at which shear on $\{121\}_R$ becomes operative. Bursill, Hyde, Terasaki, and Watanabe have observed planar boundaries on $\{101\}_R$ and have suggested that these may be shear planes.

3. Magnéli phases Ti_nO_{2n-1}

The black crystals grown by mineralisation were often very free of faults. X-ray diffraction showed the material to be multiphase, with Ti_7O_{13} and Ti_8O_{15} as major constituents, with some Ti_6O_{11}. A few crystals did show isolated planar boundaries, which were usually straight and gave fringes typical of α-boundaries [Fig. 8(a)].

Because of the low symmetry (triclinic) of these phases, electron diffraction patterns from the mixed phases could not easily be indexed with certainty in all orientations. Zones containing very short reciprocal lattice spacings were therefore sought, and such diffraction patterns could be uniquely indexed. Except that no (001) reflection was observed for the "even" oxides Ti_6O_{11} and Ti_8O_{15} (implying that Andersson's c axis should be doubled), the patterns were in agreement with the data of Andersson and Jahnberg (*18*). Such isolated planar faults as were observed were invariably perpendicular to the c^* direction—that is, they lay in $\{121\}_R$ planes, as do the shear planes that determine the structures.

Sharp spots were usually found in the diffraction patterns, but streaking parallel to c^* was sometimes observed. Planar faults and streaking represent mistakes in the sequence of shear planes, producing lamellae of other members of the series within a given crystal. Lattice fringe resolution (using (001) reflections of the shear structure superlattice) confirmed that the crystals were, in general, well ordered, without the regions of randomness present in the $TiO_{1.99}$ samples.

Boundaries between domains of Ti_7O_{13} and Ti_8O_{15} were occasionally observed within one and the same crystal. They showed little contrast and were usually detected by consideration of the diffraction patterns. One such crystal, with almost uniform contrast, gave a pattern showing the superposition of two sharply defined spacings along c^* [Fig. 9(a),(b)]. These correspond to the (001) planes of Ti_7O_{13} and (002) planes of Ti_8O_{15}; slight

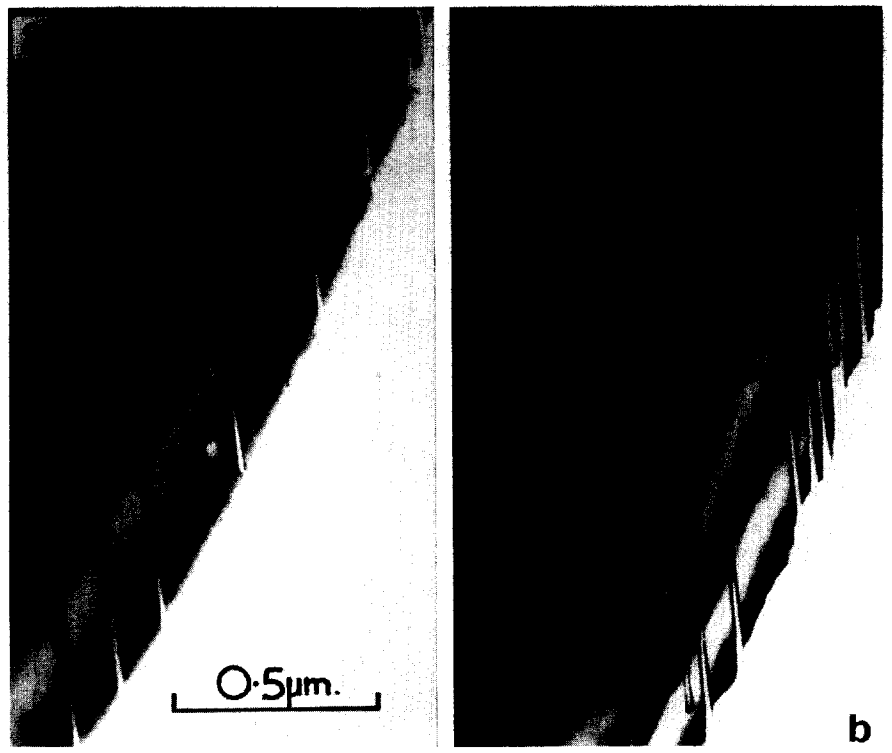

FIG. 8. (a) Isolated planar faults in Ti_7O_{13}. (b) Further faults introduced by beam heating. Magnification of (a) and (b) 75,000×.

tilting revealed a series of lamellar domains, some only 100–200 Å wide.

Unlike crystals with compositions close to TiO_2, only intense beam heating had any effect. Isolated faults could not be annealed out of the crystals but new faults could be introduced [Fig. 8(b)]. These were generally parallel to existing faults (i.e., to the structural shear planes) and were also α-boundaries, but faults at angles of 30° or 40° to these were occasionally created. As with the other materials, faults grew into the crystal from the thin edge, extending along their length, but were not seen to migrate laterally. The sharp (00l) spots became heavily streaked when a large number of faults, parallel to the shear planes, was introduced by beam heating. This growth of new faults by beam heating

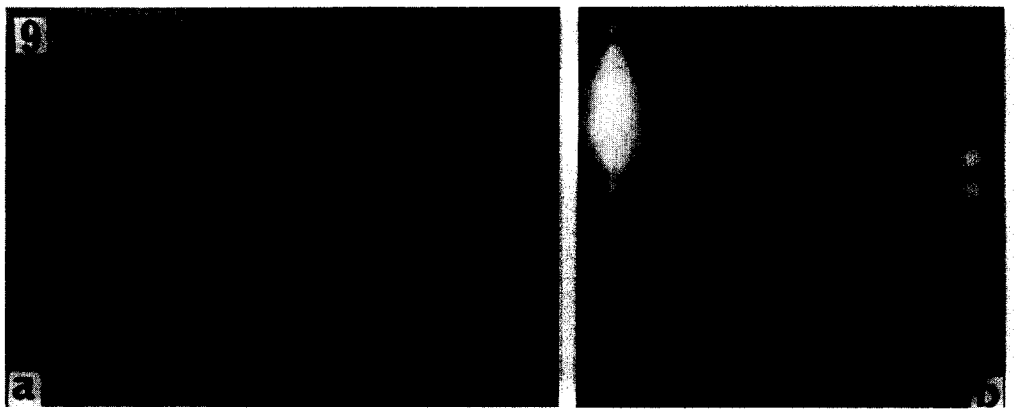

FIG. 9. (a) Lamellae of Ti_7O_{13} and Ti_8O_{15} within a single crystal grown by chemical vapour transport, 150,000×. (b) Diffraction pattern of (d) showing both periodicities. The closely spaced rows of spots are parallel to c^*.

can be attributed to a chemical reduction. The additional shear planes will define lamellae of oxygen-poorer members of the homologous series, in a nonequilibrium state. It is understandable that the faults grow in parallel to the existing shear planes, rather than on some other possible plane of shear, since there is a built-in anisotropy in the structure. Any other orientation would involve complex faulting where shear planes intersect. The occasional growth of faults at an angle to c^* was therefore unexpected. These were not fully investigated, but if they are to be identified as shear planes, they necessarily imply a double shear system of faulted blocks, not corresponding to any known family of intermediate oxides.

The existence of crystals of the kind shown in Fig. 9, with coherent domains of two component structures, reflects the small structural differences and small changes in chemical potentials between successive members of the series. It is apparent that fully coherent intergrowth can readily arise as a result of small fluctuations in the conditions during growth. In principle, regular coherent intergrowth of alternating shear plane spacings is possible (as is realised in the double shear or block structure phases (*17*), to give an almost infinitesimal gradation of composition within a series of crystallographically distinct structures. As they have been described by Andersson, and as found in this paper, the only known phases correspond to unitary stacking structures, but it may be significant that Anderson and Khan (*8*) found good evidence for a phase at $TiO_{1.82}$, midway between Ti_5O_9 and Ti_6O_{11}. This corresponds closely to the composition of a regular intergrowth of the two, with the composition $Ti_{11}O_{20}$, but microstructural evidence is lacking.

Acknowledgments

The authors express their gratitude to the Royal Society for provision of a goniometer stage, and to the Science Research Council for a Fellowship (to R.J.D.T.) which made the work possible.

References

1. J. S. ANDERSON, Thermodynamics and theory of nonstoichiometric compounds, *in* "Problems of Nonstoichiometry," (A. Rabenau, Ed.), North Holland Publ. Co., Amsterdam, 1969.
2. A. D. WADSLEY, "Nonstoichiometric Compounds," (L. Mandelcorn, Ed.), p. 98, Academic Press, New York, 1964.
3. B. C. ALCOCK, B. C. H. STEELE, AND S. ZADOR, *Proc. Brit. Ceram. Soc.* No.8 221 (1967).
4. S. ZADOR, Ph.D. Thesis, University of London, 1969.
5. S. ANDERSSON, B. COLLEN, U. KUYLENSTIERNA, AND A. MAGNÉLI, *Acta Chem. Scand.* **11**, 1641 (1957).
6. J. S. ANDERSON AND B. G. HYDE, *J. Phys. Chem. Solids*, **28**, 1393 (1967).
7. L. A. BURSILL, B. G. HYDE, O. TERASAKI, AND D. WATANABE, *Phil. Mag.* **20**, 347 (1969).
8. J. S. ANDERSON AND A. S. KHAN, *J. Less Common Metals* (1970).
9. R. GEVERS, J. VAN LANDUYT, AND S. AMELINCKX, *phys. status. solidi* **11**, 689 (1965).
10. L. A. BURSILL AND B. G. HYDE, in press.
11. K. H. G. ASHBEE, R. E. SMALLMAN, AND G. K. WILLIAMSON, *Proc. Roy. Soc. Ser. A* **276**, 542 (1963).
12. J. VAN LANDUYT, R. GEVERS, AND S. AMELINCKX, *phys. status solidi* **7**, 307 (1964).
13. J. VAN LANDUYT, *phys. status solidi* **16**, 585 (1966).
14. S. ANDERSSON AND A. D. WADSLEY, *Nature* **211**, 581 (1966).
15. M. J. WHELAN AND P. B. HIRSCH, *Phil. Mag.* **2**, 1303 (1957).
16. P. B. HIRSCH, A. HOWIE, R. B. NICHOLSON, D. W. PASHLEY, AND M. J. WHELAN, "Electron Microscopy of Thin Crystals," Butterworths, London, 1965.
17. J. G. ALLPRESS, *J. Solid State Chem.* **1**, 66 (1969).
18. S. ANDERSSON AND L. JAHNBERG, *Ark. Kemi* **21**, 413 (1963).